



THE UNIVERSITY *of* EDINBURGH

Edinburgh Research Explorer

Wave energy assessment and wind correlation for the north region of Scotland, hindcast resource and calibration, investigating for improvements of physical model for adaptation to temporal correlation

Citation for published version:

Lavidas, G, Friedrich, D & Venugopal, V 2014, Wave energy assessment and wind correlation for the north region of Scotland, hindcast resource and calibration, investigating for improvements of physical model for adaptation to temporal correlation. in *Proceedings of the ASME 2014 33th International Conference on Ocean, Offshore and Arctic Engineering OMAE 2014*. San Francisco, USA, ASME 2014 - 33th International Conference on Ocean, Offshore and Arctic Engineering, San Francisco, United States, 8/06/14.

Link:

[Link to publication record in Edinburgh Research Explorer](#)

Document Version:

Publisher's PDF, also known as Version of record

Published In:

Proceedings of the ASME 2014 33th International Conference on Ocean, Offshore and Arctic Engineering OMAE 2014

General rights

Copyright for the publications made accessible via the Edinburgh Research Explorer is retained by the author(s) and / or other copyright owners and it is a condition of accessing these publications that users recognise and abide by the legal requirements associated with these rights.

Take down policy

The University of Edinburgh has made every reasonable effort to ensure that Edinburgh Research Explorer content complies with UK legislation. If you believe that the public display of this file breaches copyright please contact openaccess@ed.ac.uk providing details, and we will remove access to the work immediately and investigate your claim.



OMAE2014-23935

**WAVE ENERGY ASSESSMENT AND WIND CORRELATION FOR THE NORTH REGION OF
SCOTLAND, HINDCAST RESOURCE AND CALIBRATION, INVESTIGATING FOR IMPROVEMENTS
OF PHYSICAL MODEL FOR ADAPTATION TO TEMPORAL CORRELATION.**

George Lavidas

Institute for Energy Systems, University of
Edinburgh
Edinburgh, Scotland, United Kingdom

Vengatesan Venugopal

Institute for Energy Systems, University of
Edinburgh
Edinburgh, Scotland, United Kingdom

Daniel Friedrich

Institute for Energy Systems, University of
Edinburgh
Edinburgh, Scotland, United Kingdom

Atul Argawal

Institute for Energy Systems, University of
Edinburgh
Edinburgh, Scotland, United Kingdom

ABSTRACT

Wave energy sites around Scotland, are considered one of the most energetic waters, as they are exposed to the Atlantic Ocean. The amount of energy reaching the shoreline provides an opportunity for wave energy deployments.

Currently, considerations on wave devices expect them to be installed at nearshore locations. That means that the potential wave resource has to be investigated, since deep to shallow water interactions alter the shape of propagated waves. Resource assessment for these regions is essential in order to estimate the available and extractable energy resource. Although several numerical models exist for wave modelling, not all are suitable for nearshore applications.

For the present work, the nearshore wave model SWAN has been used to simulate waves for the Hebridean region. The set-up, calibration and validation of the model are discussed. The resulting wave conditions are compared with buoy measurements. Results indicate that the modelling technique performed well.

INTRODUCTION

Renewable energy has experienced major development during the last 20 years; EU legislation has set ambitious targets for the penetration of renewable sources [1]. Scotland, as part of the UK has great resources in wind, both offshore and onshore and is ranked amongst richer in wave resource, with average annual wave power approaching the coast of Scotland over 60 kW/m. the bathymetric contour of Scotland is steady with no sudden downfalls [2-4]. However there have been concerns that the data provided by the Met Office wave maps present low estimations and there is constant need for revision [5].

Several studies have been conducted over the years to promote the development of wave energy, with the use of buoy data, ships and large numerical models, the results are encouraging and several technical reports have been produced that estimate the advantages and disadvantages from a wider application of renewable energy such as wind and wave [6,7].

Various authors have examined the limitation in the expansion of renewable sources and the impact that such a development may have to the energy sector. Important factors have been underlined and issues concerning mostly the intermittency of renewable sources have to be resolved [8-13].

The variability and intermittency of renewables is a factor that will limit future development of such installations, increasing the necessity for grid strengthening and infrastructure.

Thus the necessity of finding ways to reduce the variability and increase the accuracy of prediction in renewable resources, will allow us to incorporate non-fossil technologies more widely. Wind development and especially offshore is developing at fast paces, at the same time wave energy devices have started to become efficient and economic incentives are given for their development [11,14].

Numerical wave models can reproduce sea states but a rigorous effort has to be made in order for the model to provide us with wave field that correspond to real data, several simulations and calibration states have to be preceded in order for a model to perform correctly.

Main interest of this paper is to introduce the investigation, calibration and validation of the simulation. Producing accurate simulated waves will allow assessing the temporal correlation and investigate the probabilities in energy generation.

NUMERICAL MODELLING

From the early starts of wave resource assessment, it was evident that wind is the most important factor affecting generation and propagation of waves. Amongst the first observations of waves is the Airy theory for small amplitude waves in a finite environment [15-17], since then many improvements have been introduced, proving that the understanding of waves is a challenging and difficult task [18].

Real waves though don't follow linear theory, but instead in order to predict wind generated waves more complex non-linear models have to be taken into account. With the increase of computational strength in computers we were able to develop several numerical models that simulate wind generated seas.

Especially in shallow waters non-linear interactions affect propagation and the final incoming flux. Several models have been developed throughout the years with different numerical solutions approaches for wave simulations.

Currently we are into the third generation models with WAM, and WaveWatch III (WWIII) used for coarser and large scale predictions while for nearshore application SWAN, TOMAWAC and MIKE21 are typically preferred [19].

Although differences exist between the numerical models, often they are categorized as deterministic (phase resolving, in time domain or spectral domain) and stochastic (phase averaged) models.

SWAN is a phase average model chosen based on the way it resolves the action balance equation, whereas relative radian frequency (σ) and the ability it has to incorporate shallow water parameters [20-22]. The solution may be either time dependent or non-time dependent. As seen in Equation

(1) the wave kinematic equation is being solved for a non-stationary run with (t) representing the time component, (N) the action density spectrum.

$$\frac{\partial N(\sigma, \theta; \lambda, \varphi, t)}{\partial t} + \frac{\partial C_{g, \lambda} N(\sigma, \theta; \lambda, \varphi, t)}{\partial \lambda} + (\cos \varphi)^{-1} \frac{\partial C_{g, \varphi} N(\sigma, \theta; \lambda, \varphi, t)}{\partial \varphi} + \frac{\partial C_{\theta} N(\sigma, \theta; \lambda, \varphi, t)}{\partial \theta} + \frac{\partial C_{\sigma} N(\sigma, \theta; \lambda, \varphi, t)}{\partial \sigma} = \frac{S(\sigma, \theta; \lambda, \varphi, t)}{\sigma} \quad (1)$$

Latitude (φ), longitude (λ), propagation velocities (C), provide us with the solution of the action balance equation for two dimensional spectrum in spherical coordinates system and S_{tot} is the source term allows the user to activate various components as seen in Equation 2.

$$S_{tot} = S_{in} + S_{nl3} + S_{nl4} + S_{ds,w} + S_{ds,b} + S_{ds,br} \quad (2)$$

Whereas in Equation (2) wind input S_{in} , triads S_{nl3} , quadruplet S_{nl4} interactions, Whitecapping $S_{ds,w}$, bottom friction $S_{ds,b}$ and $S_{ds,br}$ depth breaking. What separates SWAN is the ability to activate shallow water interactions, triads, allowing to reproduce better the final waves in shallow regions [20].

The wind induction used, is the sum of linear and exponential growth, based on the fact that wave generation is described as a resonance mechanism between wind and the distortion of sea surface. When S_{in} is used quadruplets S_{nl4} have to be used, allow showing the continuous shift of frequency from waves.

The last three terms whitecapping, bottom friction and depth breaking consist the often mentioned dissipation term. By breaking down that term in components, the solution allows us to simulate the effects of shallow water regions.

One of the most important input terms is the S_{nl3} , triad interactions which account for the shallow water effects and enhance the ability of SWAN to be used for nearshore application.

APPLICATION OF MODEL

The area under investigation is located to the North West of Scotland the Isle of Lewis, and surrounding waters known also as Outer Hebrides.

The issues investigated predominately are wind generated waves, data used for the construction of input wind files, and computational grids were obtained by NOAA and ECMWF. [23-25].

For this study SWAN cycle III 40.91ABC version was used. As mentioned above the input grids were obtained and converted into appropriate input format, after several attempts

in order to maximize resolution and at the same time keep computational time at acceptable levels.

First step for the simulation is the selection of the area and the grid generation, for that purposes we chose a grid that has 6 degrees longitude (11West to 5East) and 5.5 degrees latitude (61North to 55.5 North). The grid selected was converted into a structured form with a resolution 0.025x0.025, leading to 241 points of longitude and 221 points in latitude.

A fine resolved grid, allows for the dissipation terms of Equation (2) to be applied better. Depth breaking, dissipation and triads are connected to the depth and the resolution of the input file.

Although it has to be added, that in the case of the structured grids a very fine resolution will lead to the increase of the computational time. This factor has to be taken into account when considering the construction of the mesh, since we investigate shallow waters the desirable resolution must be focused on those areas.

In the case that a bigger finer grid is to be implemented the option of nesting SWAN into a coarser grid should be considered, but that will increase the computational requirements

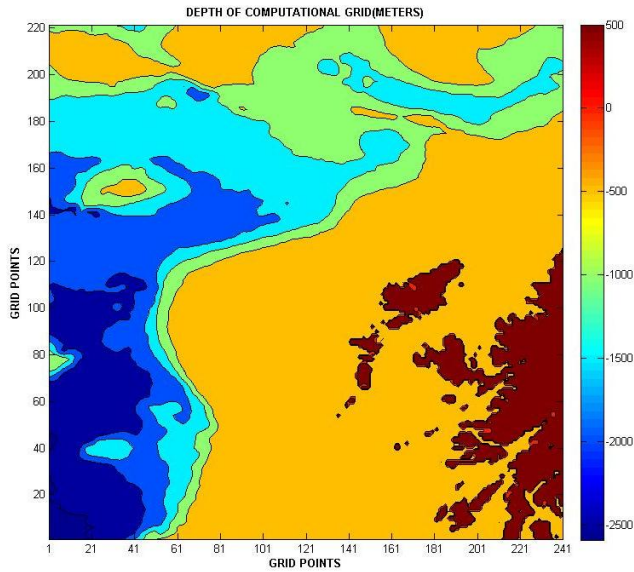


FIGURE 1: depth of computational grid in meters

Initial spectral elements for the simulations have to be set, for this area, and after an initial screening the minimum real frequency was designated. SWAN requires some spectral information, although the both minimum and maximum frequencies can be set arbitrary set by the user or by experience. It is desirable to set a minimum discrete frequency, so that the simulated waves will have a good initial approximation for generation. Minimum discrete frequency is set to 0.04 Hz and 24 bins are assigned. Spectral

directions are considered into a full circle and are assigned in 36 bins.

Boundary conditions for this run used previous recorded data of H_s (significant wave height), T_p (peak wave period), P_kDir (peak wave direction) and directional spreading (D_{spr}). The time domain for these data extended beyond the timeframe of interest so as to have a better representation for the boundary interaction into the temporal domain that was finally chosen.

Recorded measurements for the Sea First buoy were obtained by the CEFAS portal and the overall environmental conditions used are extrapolated by WaveWatch III and ERA-Interim [24-26] allowing us to cross-correlate the accuracy of the simulation.

Wind input was constructed by using values from ECMWF, the required quantities in order to construct a correct input file, are U_{10} wind speed and V_{10} wind profile. The grid for these quantities was the same as the bathymetry, although SWAN will also accept wind input grids that extent the computational domain as well.

The construction for the wind input is of significance, if the S_{in} term is to be utilized correctly and wind induced waves are to be generated. For every grid point of the computational mesh U_{10} and V_{10} have to be provided. For every point of the grid two values describing the wind resource are required. The resolution of the wind was 0.125° by 0.125° with a discrete timestep of 6 hours.

The buoy is located at 7.9° West and 57.2° North, and it is active since 23-Feb-2009, able to record H_{sig_buoy} , T_{p_buoy} (Dominant wave period in sec), T_{m02_buoy} (average zero crossing period), P_kDir_buoy (Peak direction) in degrees and directional spreading D_{spr_buoy} (degrees), these data are to be used in order to calibrate and correlate the accuracy of our model.

Moreover corresponding wind and wave data obtained by ECMWF ERA Interim re-analysis package, for the same location of the buoy and their values are compared with the buoy and SWAN [24].

HINDCAST AND VALIDATION

In order to simulate the wave conditions accurately proper physical of waves have to be given, nautical convection is considered, meaning that waves are generated and propagated from the side the wind is originating [26].

For the definition of the simulated spectra shape the JONSWAP will be used. Usually in numerical modelling applications there are two distinct options for the shape of spectra the JONSWAP and the Pierson-Moskowitz (PM), their main differences is that the PM accounts for fully developed seas while JONSWAP includes a (γ) gamma parameter that corresponds better to not-fully developed sea states.

Whitcapping has been included and the alternative formulation and options mention at [27] have been investigated with the most suitable combination in use.

Turning rates and frequency shifting limiters have been adjusted as proposed [28].

Quadruplets have been applied, due presence of wind with appropriate values, triads have been turned on to represent the frequency exchange due to the propagation of waves to shallower regions.

Simulation computational time interval was set to 30 minutes, when using a numerical model it is important for the user to first select an appropriate time step based on the resolution of the input meshes and their timestep. The interval then has to be lowered in order to acquire a better resolved output.

Numerical simulations, although often are fed initial conditions and spectral properties as described, user must also provide a sufficient ‘warm-up’ period to be set and avoid errors that may be carried through resulting in abnormal wave generation.

The optimal solution is to extend the simulation’s computational time from a past timestep to fully develop the wave field. If this is not followed then the initial, often erroneous, calculations will alter the results.

As prescribed for a non-stationary run additional time, will allow for the spectral and physical properties to smooth out the initial calculations and will return output that will correspond to actual sea states.

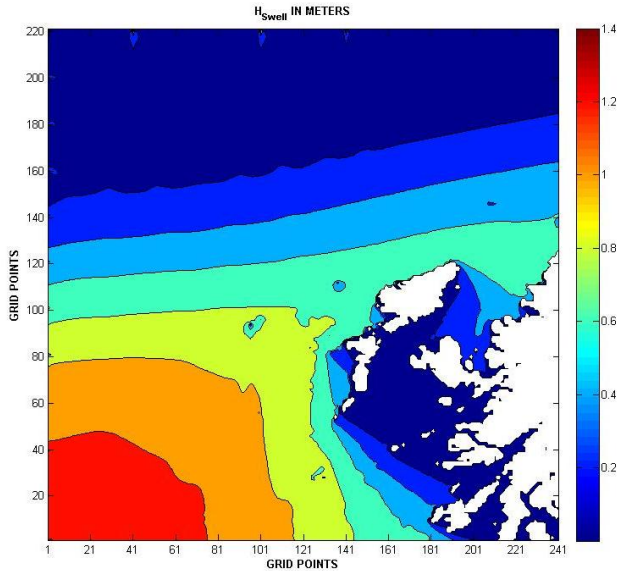


FIGURE 2: Swell propagation for the last timestep in meters

From Figures 9-12, in ANNEX A, we can see that the simulated wind generated waves have followed the trends of the observed data with some discrepancies and clearly an under-estimation of the highest peaks, while the convergence in Figure 4 appears to have a decreased accuracy. Following the graphical representation and identification of the trends,

the data undertook a comparison that pointed out the deficiencies of the model.

Additional information and more extensive presentation of the simulated wave of the computational grid can be found in ANNEX A.

A quantitative approach and evaluation of the results the rms_{error} , Scatter Index (SI), correlation coefficient (R), Operation Performance Index (OPI), and bias of the measurements are considered. This approach will allow evaluating the process and identifying errors and restrictions[29-30].

TABLE 1: SWAN performance

	H_{sig} (m)	T_p (sec)	T_{m02} (sec)	P_kDir (°)
R	0.96	0.96	0.97	0.92
SI	0.31	0.35	0.30	0.40
rms_{error}	0.83	3.6	1.9	107.3°
Av.buoy	2.66	10.4	6.63	268°
Av.SWAN	2.16	8.2	5.16	248°
OPI	0.31	0.34	0.30	0.40
Bias	-0.5	-4.2	-1.47	-20°

It is obvious that the simulations have produced a wave field that follows the trend of the actual data but under-estimations are located at the peaks. The simulation has reproduced the trend and generation of wind waves in the computational grid. The correlation R is stating clearly that the physical processes reproduced by the simulation follow the real wave field that is encountered.

These divergences of the buoy data and the simulations can be attributed to the length of the computational grid, the level of complexity that the local sea has and the time resolution of the input wind.

Based on the computational grid and its characteristics it can be stated that the sea conditions are fairly complex. When assessing the quantitative results from a wave simulation [29] different things should be considered. In the case of complex seas a high H_{sig} rms_{error} appear logical and acceptable but always bearing in mind the average value of H_{sig} . In addition a very high rms_{error} with a lowered average may lead to an increase of the scatter index above 50%, in this case though the average of the simulation is good thus the SI is lowered.

The biases recorded are low, while the SI index shows that the distribution of the values is not wide. Total convergence is difficult to be achieved though, as mentioned SWAN is a phase average solution which provided us highly correlated waves for the majority of the measurements, although some areas are poorly represented. In order to assess the validity of the simulation several considerations have to be taken into account.

Depending on the scale of the application, large or small scale, SWAN is known to produce unstable and underestimated results [31], mainly due to the length of the

computational grid and the DIA (Discreet Interaction Approximation) method used in the SWAN source code. Generally DIA approximation favours the lower frequency spectrum and widens the directional spreading.

Another factor affecting the simulation results is the wind time resolution of computational grid and the input time step, in our simulation a 6 hour timestep was used, based on previous research and observation it is underlined that due to the time resolution from the ECMWF data, underestimation of real peaks and over-estimation of troughs is something to be expected and will affect the final results and performance index of the model (OPI) [32-33].

Improvements in the time resolution of a dataset are expected to enhance the under-estimated maxima, and also add to the minimum values. Acquiring though datasets with both fine spatial and temporal (short timestep) resolution are hard to be acquired.

ECMWF wind data have been scrutinized over the years and although their temporal resolution available is considered adequate, 6 hour, they only have a 5% under-estimation of strong wind fields thus leading to the corresponding waves [33].

Specifically for SWAN under-estimation/overestimation, along with diffusion in biases were reported for simulations at the Black Sea [34] with a usual underestimation of peaks at 50%, while [29] similar trends have been recorded in the performance of SWAN for low T_p values assigning greater importance to the OPI index and the bias that exists within the simulations, rather than the actual R^2 index.

Also a comparison with the ECMWF point that corresponds to the buoy was isolated, showing us that the simulation has proven able to attain the wave generated trend although the peaks are still underestimated in the ECMWF re-analysis.

The time domain of the simulation and its generation coincides with the measured data obtained by the buoy, as [32] stated there seems to be a connection between the wind speed time resolution which often results into the depreciation of H_{sig} , the R as seen in Table 1 the correlation coefficient from the SWAN simulation is 0.96.

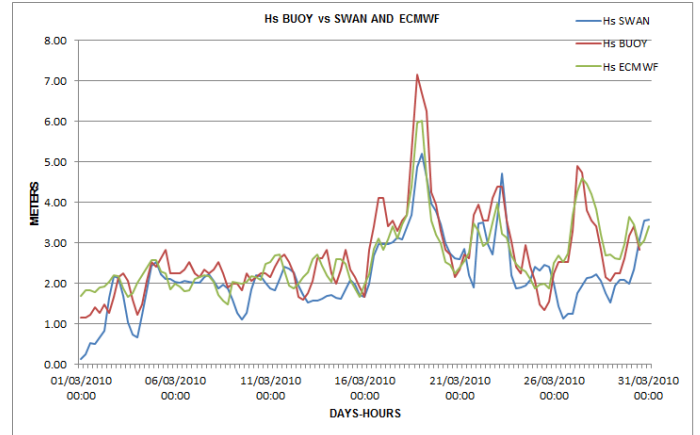


FIGURE 3: Comparison of H_s acquired by the buoy, ECMWF and SWAN.

ECMWF wave simulations are performed by applying the WAM cycle 4 numerical modelling approach, the data produced are a constant results of often nested runs, that allows a good representation of the wave field, since the previous run are used for re-analysis. This way ECMWF is able to reproduce boundaries for all the points of an area, for any mesh resolution and grid points number [24-33].

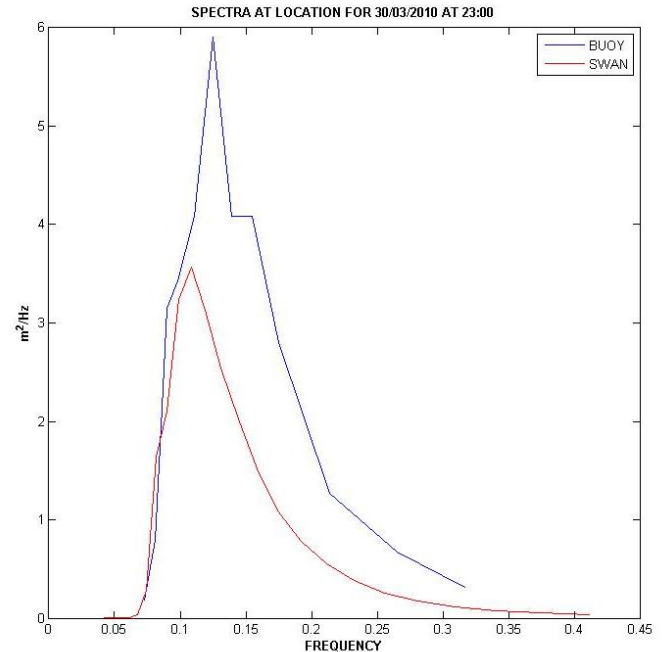


FIGURE 4: 1D wave spectra compared

The spectra obtained by the simulation, have similar trends with the real spectrum obtain for the same time step at the same location.

The maxima in the spectra are located at neighbourly frequency areas, the difference shown can be attributed to the underestimation provided in the previous sections.

The difference though in the location of the frequency value corresponding to the discretization of the frequencies set and used. The selected minimum frequency was an approximation based on the corresponding resource assessment for the same month by data obtained from the buoy.

Simulated spectrum are peaking at approximately 0.1 Hz while the buoy obtained at 0.125Hz, this can be attributed to the bins categorizing we have set.

The peak spectrum is obtained with small difference to both frequency and energy content. The trends of the spectrum are similar with difference at peaks located at slightly different frequencies.

CONCLUSIONS

The main focus of this calibration investigation was to examine the wind generated waves and how we can connect them with the wind resource, results produced by SWAN simulations have shown that trends follows the general wind-wave generation pattern with some underestimation due to the time resolution of the data. Further work with smaller temporal resolution than the current used is to be performed, to further improve the findings.

Finer temporal resolutions of the data especially wind and boundaries will allow increased accuracy, helping the convergence of the quantities produced and compared with the buoy.

Based on the calibration of the model and the fact that the physical properties are represented satisfactory by SWAN the future work will include the attainment of more detailed data for the simulation of the wave field. Since the correlation factors obtained by the calibration run show us that the physical set-up of the model operates, the use of detailed data is expected to increase the overall simulation and correct the faults that were observed, allowing an attempt to temporally correlate the properties in the best way possible.

More realistic spectra will attempt to be obtained, not only satisfying the trend but the magnitude as well. Then they shall be compared with buoy and theoretical spectrum estimations. The physical dependence of waves on wind has been confirmed by previous studies and theoretical approaches, although the expectation of the approaching spectra seems to differ as wave propagates.

Most errors can be traced back to the lack of input data sources and their resolution both temporal and spatial. The difficulties in acquiring buoy data for the correlation and comparison is an important issue. Nevertheless even in absence of multiple buoys, generation and approximation of wave fields can be produced by SWAN with high correlations.

In lack of reference points the user has to rely on reducing the overall SI and the bias of the simulation, discrepancies are

more often met for the periods, although this is partially attributed to boundaries, minimum and maximum selection of the frequency bins.

Another factor taken into account is the insertion of boundaries for the computations, unfortunately not many publically available buoys exist around the Atlantic that are able to produce data for different locations, thus the necessity for accessing global wave models is imperative.

Freely available data include wave and swell height, it is important to underline that wave periods often provided are not in the appropriate form.

Usually average energy periods T_e are given and the conversion into T_z and T_p is required. Directional spreading is one of the key elements that is also often not provided by freely available databases thus the conversion has to be based on wave theory.

Available wind resources are able to simulate sea states and wind generated waves, but if a simulation is to be performed to open seas such as the Atlantic, then good approximated boundaries have to be included and a finer temporal resolution wind input have to be sought out.

With increasing the available timesteps used, reducing the time interval, we will be able to detect the variances of seas better and provide the important elements of boundaries and wind input in better detail, allowing an increase for the computational accuracies.

Finally SWAN offers several alterations that affect the outcome, several changes have been proposed within the text, but the user has to be able to choose the best choice for the area under investigation. Often times the most important issues that have to be lowered are the friction parameters and the level for the computed accuracy of estimated waves by SWAN that enter our area, has to be increased.

ACKNOWLEDGMENTS

The author would like to thank the EPSRC for the funding opportunity, ECMWF, NOAA, CEFAS for providing the data, SWAN development team that provides and constantly updates the source code of SWAN.

REFERENCES

- [1] E. Parliament, "The European Parliament. Directive of the European Parliament and of the Council on the promotion of the use of energy from renewable sources amending and subsequently repealing directives 2001/77/ec and 2003/30/ec.," 2009.

- [2] J. Cruz, Ed., *Ocean Wave Energy: Current Status and Future Perspectives*. 2008.
- [3] D. for Business & Enterprises, “Renewable Atlas of marine Renewable sources (2012),” *Atlas of marine Renewable sources*, no. March, 2008.
- [4] S. Barstow, G. Mørk, L. Lønseth, and J. P. Mathisen, “WorldWaves wave energy resource assessments from the deep ocean to the coast,” *Fugro OCEANOR AS*, pp. 149–159.
- [5] Carbon Trust and AMEC, “Carbon Trust Foreword to UK Wave Resource Study .,” *carbon trust*, no. October, 2012.
- [6] A. F. D. O. Falcão, “Wave energy utilization: A review of the technologies,” *Renewable and Sustainable Energy Reviews*, vol. 14, no. 3, pp. 899–918, Apr. 2010.
- [7] J. Taylor, R. Wallace, and J. Bialek, “Matching Renewable Electricity Generation with Demand,” *Scottish Executive*, no. February, 2006.
- [8] Y. Krozer, “Cost and benefit of renewable energy in the European Union,” *Renewable Energy*, vol. 50, pp. 68–73, Feb. 2013.
- [9] DTI, “Quantifying the system cost of additional renewables in 2020,” *October*, no. October, pp. 1–130, 2002.
- [10] G. Richards, B. Noble, and K. Belcher, “Barriers to renewable energy development: A case study of large-scale wind energy in Saskatchewan, Canada,” *Energy Policy*, vol. 42, pp. 691–698, Mar. 2012.
- [11] B. V. Mathiesen, H. Lund, and K. Karlsson, “100% Renewable energy systems, climate mitigation and economic growth,” *Applied Energy*, vol. 88, no. 2, pp. 488–501, Feb. 2011.
- [12] J. K. Kaldellis and M. Kapsali, “Shifting towards offshore wind energy—Recent activity and future development,” *Energy Policy*, vol. 53, pp. 136–148, Nov. 2012.
- [13] M. a. Delucchi and M. Z. Jacobson, “Providing all global energy with wind, water, and solar power, Part II: Reliability, system and transmission costs, and policies,” *Energy Policy*, vol. 39, no. 3, pp. 1170–1190, Mar. 2011.
- [14] A. B. Melo and J. Huckerby, “Annual Report 2012, Implementing Agreement on Ocean Energy Systems (OES-IA),” *Ocean Energy Systems (OES-IA)*, 2012.
- [15] D. Toke, “The UK offshore wind power programme: A sea-change in UK energy policy?,” *Energy Policy*, vol. 39, no. 2, pp. 526–534, Feb. 2011.
- [16] J. Tucker, M., *Waves in Ocean Engineering Measurements, Analysis, Interpretation*. Ellis Horwood Ltd., 1991.
- [17] I. . Young, *Wind Generated Ocean Waves-volume 2*, 1st ed. Elsevier Ocean Engineering Book Series, 1999.
- [18] B. Kinsman, *Wind Waves their generation and propagation on the Ocean Surface*, Dover edit. Englewood Cliffs, N.J: Prentice-Hall, 1965, pp. 1–676.
- [19] L. Cavaleri, J.-H. G. M. Alves, F. Ardhuin, A. Babanin, M. Banner, K. Belibassakis, M. Benoit, M. Donelan, J. Groeneweg, T. H. C. Herbers, P. Hwang, P. a. E. M. Janssen, T. Janssen, I. V. Lavrenov, R. Magne, J. Monbaliu, M. Onorato, V. Polnikov, D. Resio, W. E. Rogers, A. Sheremet, J. McKee Smith, H. L. Tolman, G. van Vledder, J.

- Wolf, and I. Young, “Wave modelling – The state of the art,” *Progress in Oceanography*, vol. 75, no. 4, pp. 603–674, Dec. 2007.
- [20] V. Venugopal, T. Davey, H. Smith, G. Smith, L. Cavaleri, L. Bertotti, and L. John, “Equitable testing and evaluation of Marine Energy Extraction Devices of Performance, Cost and Environmental Impact. Deliverable 2.3 Application of Numerical Models,” 2010.
- [21] L. H. Holthuijsen, *Waves in oceanic and coastal waters*. Cambridge University Press, 2007.
- [22] N. Booij, R. C. Ris, and L. H. Holthuijsen, “A third-generation wave model for coastal regions: 1. Model description and validation,” *Journal of Geophysical Research*, vol. 104, no. C4, p. 7649, 1999.
- [23] A. Akpinar and M. İ. Kömürçü, “Wave energy potential along the south-east coasts of the Black Sea,” *Energy*, vol. 42, no. 1, pp. 289–302, Jun. 2012.
- [24] E. C. for M. R. W. F. ECMWF, “ERA Interim,” 2013. [Online]. Available: <http://www.ecmwf.int/>.
- [25] N. G. D. C. NOAA, “Grid extraction ETOPO1,” 2013. [Online]. Available: <http://maps.ngdc.noaa.gov/viewers/wcs-client/>.
- [26] F. & A. S. CEFAS, Center for Environment, “CEFAS,” 2013. [Online]. Available: <http://www.cefasc.defra.gov.uk/home.aspx>.
- [27] T. Delft, *User manual SWAN Cycle III version 40.91ABC*. Delft University of Technology Faculty of Civil Engineering and Geosciences Environmental Fluid Mechanics Section, 2013.
- [28] W. E. Rogers, P. Hwang, and W. D. Wang, “Investigation of Wave Growth and Decay in the SWAN Model : Three Regional-Scale Applications,” *Physical Oceanography*, pp. 366–389, 2002.
- [29] J. C. Dietrich, M. Zijlema, P.-E. Allier, L. H. Holthuijsen, N. Booij, J. D. Meixner, J. K. Proft, C. N. Dawson, C. J. Bender, A. Naimaster, J. M. Smith, and J. J. Westerink, “Limiters for spectral propagation velocities in SWAN,” *Ocean Modelling*, Nov. 2012.
- [30] R. C. Ris, L. H. Holthuijsen, and N. Booij, “A third-generation wave model for coastal regions: 2.Verification,” vol. 104, pp. 7667–7681, 1999.
- [31] G. J. Komen, L. Cavaleri, M. Donelan, S. Hasselmann, and P. A. E. . Janssen, *Dynamics and Modelling of Ocean waves*. Cambridge University Press, 1994.
- [32] T. Delft, *Scientific and technical documentation SWAN cycle III version 40.91ABC*. 2013.
- [33] L. Cavaleri, “Wave Modeling—Missing the Peaks,” *Journal of Physical Oceanography*, vol. 39, no. 11, pp. 2757–2778, Nov. 2009.
- [34] A. Sterl, G. J. Komen, and P. D. Cotton, “Fifteen years of global wave hindcasts using winds from the European Centre for Medium-Range Weather Forecasts reanalysis: Validating the reanalyzed winds and assessing the wave climate,” *Journal of Geophysical Research*, vol. 103, pp. 5477–5492, 1998.

ANNEX A

SWAN simulation wave field results

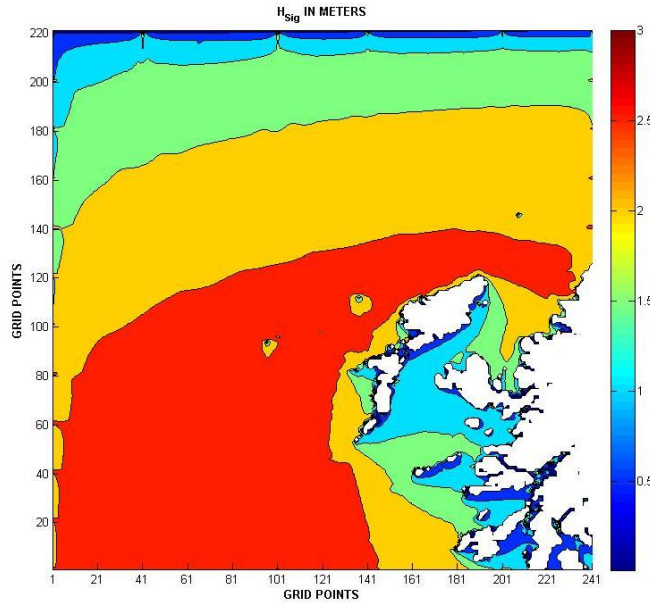


FIGURE 5: Significant wave height at last computational step

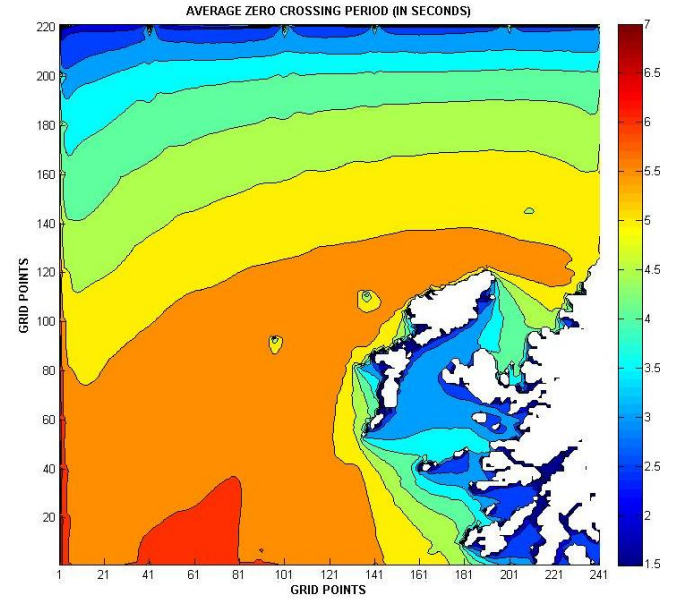


FIGURE 7: Average crossing period at last computational step, in seconds

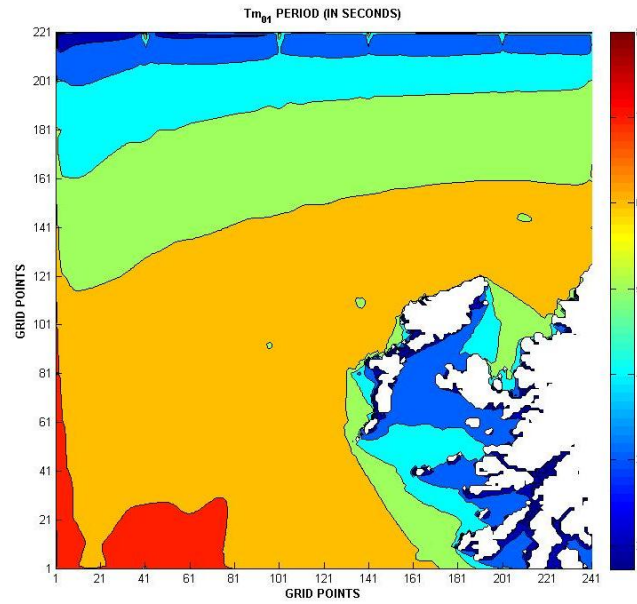


FIGURE 6: Peak period at last computational step, in seconds

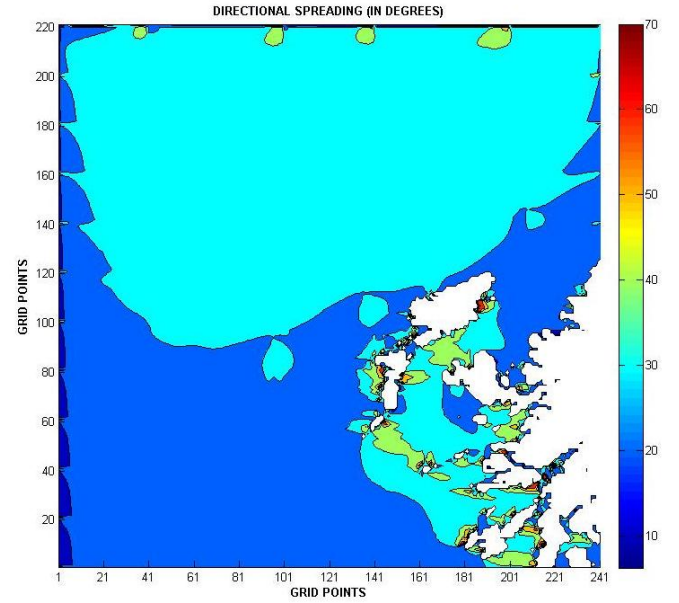


FIGURE 8: Directional at last timestep in degrees

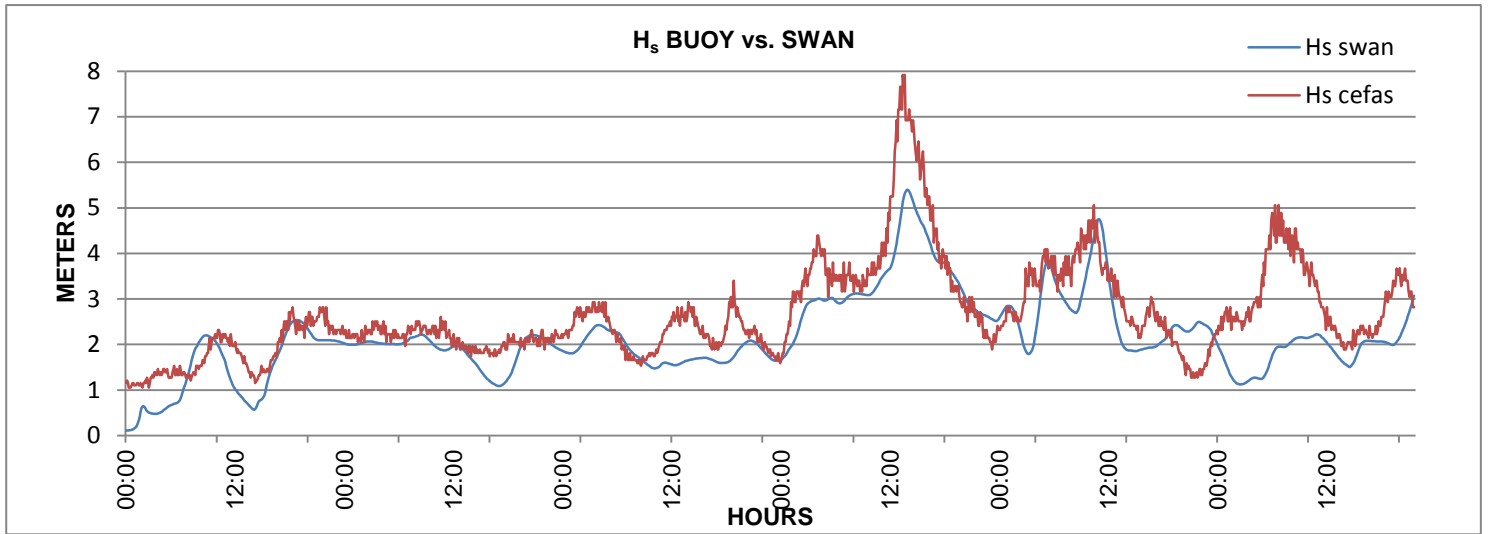


FIGURE 9: Wave height compared from data of the cefas buoy and SWAN, in meters

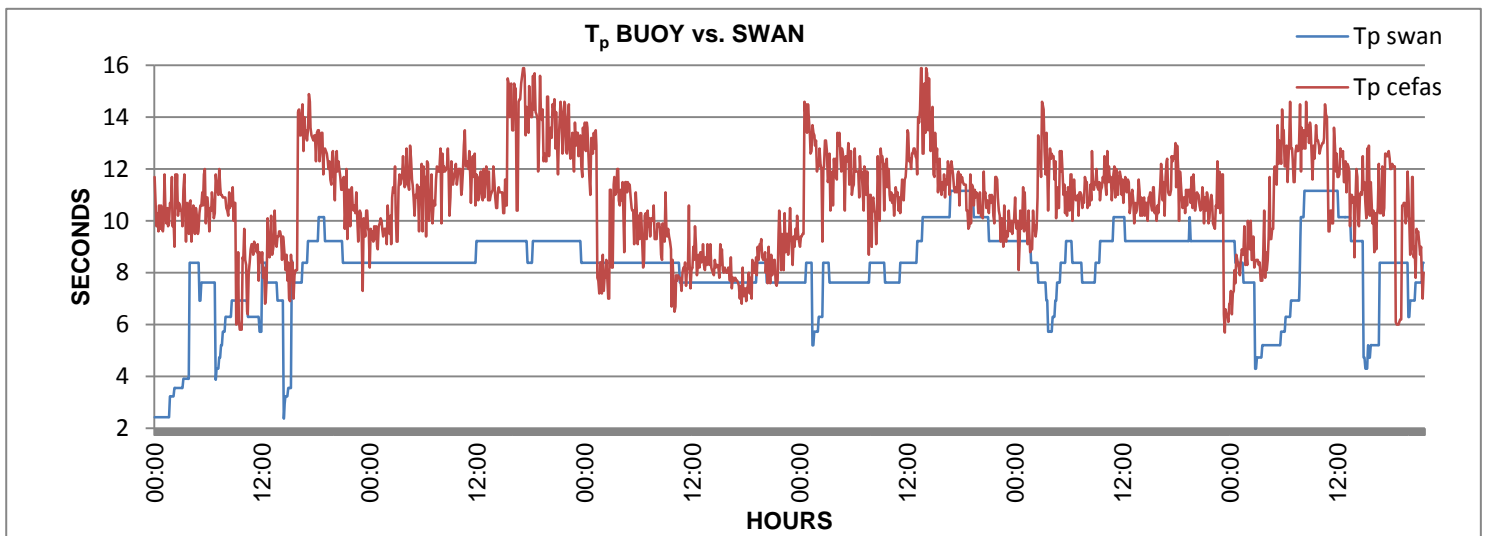


FIGURE 10: Peak period of buoy and SWAN, in seconds

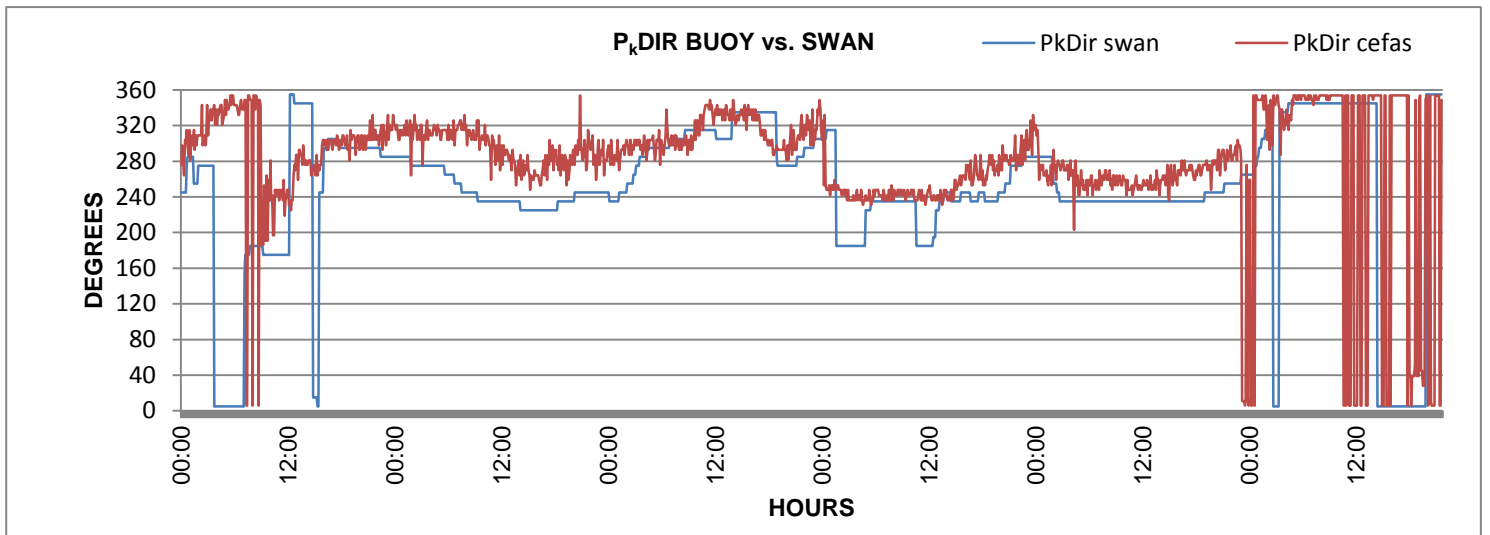


FIGURE 11: Peak wave direction between buoy and SWAN in degrees

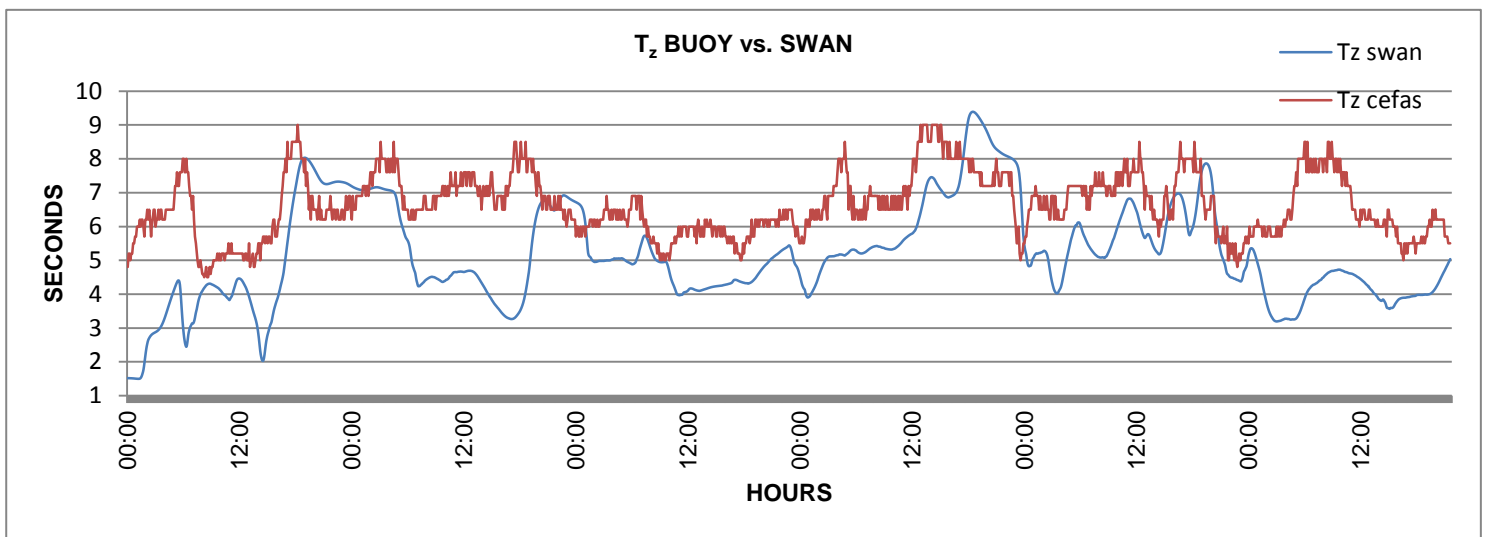


FIGURE 12: Average zero crossing period between buoy and swan in seconds